Chapter 8

In-vivo Biodistribution and Scintigraphy Studies

8. In-vivo STUDIES

8.1 Introduction

The study of the *in-vivo* behaviour is very critical for the successful development of the liposomal formulations. The tumor targeting ability of the formulations can well be established by carrying out the experiments in tumor bearing animal model. Studies of the pharmacokinetics of the formulations in suitable animal models during the later stages of development are crucial for attainment of the desired product performance. This particularly true in case of pH sensitive long circulating liposomes where in-vitro testing may not necessarily indicate the in-vivo performance of the formulation. However, in all cases, suitable *invitro-invivo* correlations can be established. Inclusion of these in-vitro tests in the quality assurance programme of the formulation can then be done so as to ensure that each batch will meet the criteria required for successful in-vivo performance. These studies are also crucial for the systems which are being investigated for the first time since new *in-vivo* distribution patterns can reveal the way for new vistas in the cancer therapy.

8.2 EXPERIMENTAL

Selection of animals

Balb/c mice of either sex, of 2-3 months old, weighing between 20-25 g was chosen for blood kinetic study of the drugs and their liposomal formulations. No diet restriction was enforced prior to studies. 3 mices were taken for the study in each time point of particular group.

Balb/c male mice, of 2-3 months old, weighing between 20-25 g with Ehrlich Ascites tumor (EAT) developed in the right thigh region were chosen for biodistribution and tumor uptake studies of the drugs and their liposomal formulations. No diet restriction was enforced prior to studies. 6 mices were taken for the study in each group.

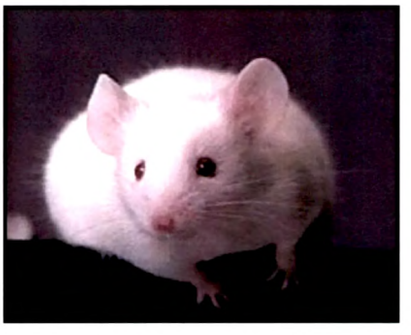

Figure 8.1. Balb/c mice

Tumor implantation

Ehrlich Ascites Tumor (EAT) was maintained in the peritoneum of the mice in the ascites form by serial weekly passage. Exponentially growing EAT cells were harvested, washed and resuspended in phosphate buffered saline and about 1.5 x 10^7 cells were injected intramuscularly in the thigh of the right hind leg of the mice of 2-3 months old age mice weighing 25-30 g. After 8-10 days a palpable tumor in the volume range of 0.9 ± 0.1 cm^3 was observed and used for further studies.

8.3 Blood kinetic studies

Balb/c mice were administered with 2 millicurie of labeled complex through tail vein using a syringe with 26" gauze needle. At different time intervals, about 0.5ml of blood samples were withdrawn from the direct cardiac puncture and the radioactivity was measured using a gamma counter calibrated for Tc-99m energy. An amount equal to 7.3% of the body weight was considered to represent whole body blood and data were expressed as percent administered dose at each time interval (Wu et. al., 1981)

Table 8.1. Blood Kinetics of Paclitaxel

Time (h)	% Injected Dose		
	PCL	CLPT	PSPT
0.25	13.98 ± 2.45	21.34 ± 2.03	39.78 ± 1.98
0.50	12.43 ± 2.12	20.12 ± 1.74	36.67 ± 1.55
1	8.12 ± 1.94	17.08 ± 1.83	34.13 ± 1.68
2	4.02 ± 1.32	12.45 ± 1.34	31.96 ± 0.82
4	2.03 ± 0.76	10.46 ± 0.93	28.02 ± 1.06
6	0.91 ± 0.42	5.74 ± 1.01	24.69 ± 1.11
24	0.03 ± 0.01	1.88 ± 0.41	15.47 ± 0.71
48	0.00 ± 0.00	0.00 ± 0.00	8.63 ± 0.48

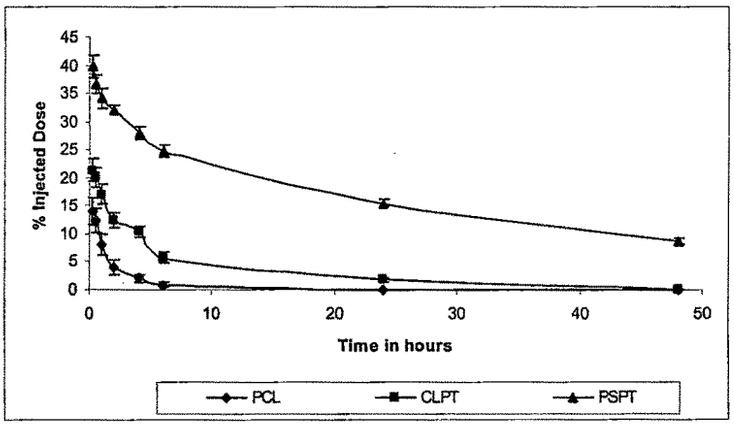

Figure 8.2. Pharmacokinetics of ^{99m} Tc-labeled of Paclitaxel and its liposomal formulations after intravenous injection into tail vein of Balb/c mice.

Table 8.2. Comparative pharmacokinetic parameters of Paclitaxel and its liposomal formulations after i.v. injection in Balb/c mice (upto 48 hours).

	C_{max} (µg/ml)	T_{max} (h)	AUC $_{0-48}$ (µg.h/ml)	$AUC_{0-\infty}$ (µg.h/ml)	$T_{1/2}$ (h)	λ_z (K_{el}) (1/hr)	MRT last (h)	$V_{d\ obs}$ (ml/kg)	Cl_{obs} (ml/hr/kg)
PCL	13.98	0.25	35.67	35.82	3.43	0.2024	2.77	13.80	2.79
CLPT	21.34	0.25	142.43	165.45	8.48	0.0817	6.24	7.40	0.60
PSPT	39.78	0.25	834.00	1179.35	27.74	0.0250	17.51	3.39	0.08

Table 8.3. Blood Kinetics of Irinotecan Hydrochloride

Time (h)	% Injected Dose		
	IH	CLIH	PSIH
0.25	15.06 ± 2.66	24.67 ± 2.14	38.64 ± 2.94
0.50	12.75 ± 2.43	21.03 ± 1.88	35.38 ± 1.46
1	8.44 ± 1.84	17.86 ± 2.04	32.08 ± 2.42
2	4.11 ± 1.28	13.09 ± 1.64	30.66 ± 0.56
4	1.86 ± 0.58	10.14 ± 0.82	27.18 ± 1.56
6	0.76 ± 0.26	6.54 ± 1.18	23.90 ± 1.06
24	0.02 ± 0.01	2.02 ± 0.40	12.74 ± 0.84
48	0.00 ± 0.00	0.00 ± 0.00	6.78 ± 0.59

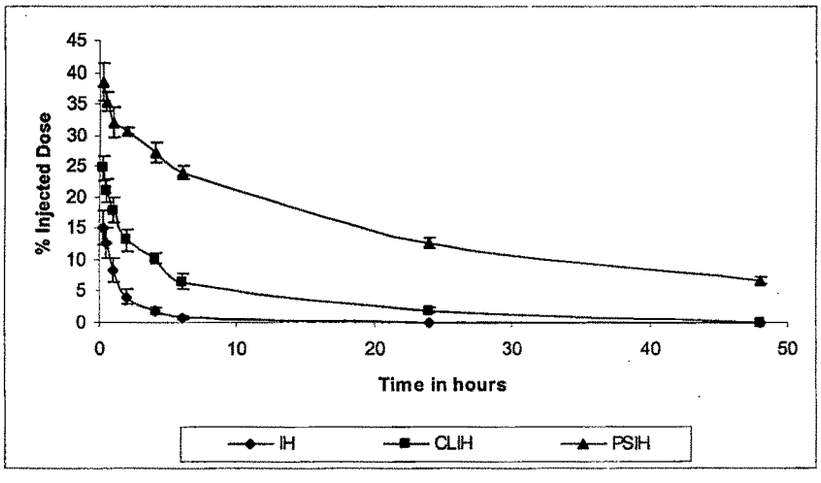

Figure 8.3. Pharmacokinetics of ^{99m}Tc-labeled of Irinotecan and its liposomal formulations after intravenous injection into tail vein of Balb/c mice.

Table 8.4. Comparative pharmacokinetic parameters of Irinotecan and its liposomal formulations after i.v. injection in Balb/c mice (upto 48 hours).

	C_{max} (µg/ml)	T_{max} (h)	AUC_{0-48} (µg.h/ml)	$AUC_{0-\infty}$ (µg.h/ml)	$T_{1/2}$ (h)	λ-Z (K_{el}) (1/hr)	MRT last (h)	$V_{d\ obs}$ (ml/kg)	Cl_{obs} (ml/hr/kg)
IH	15.08	0.25	34.82	34.91	3.20	0.2172	2.50	13.19	2.86
CLIH	24.67	0.25	154.56	179. 78	8.65	0.0801	6.26	6.94	0.56
PSIH	38.64	0.25	740.51	958.15	22.25	0.0312	16.34	3.35	0.10

8.4 Biodistribution and tumor uptake studies

Biodistribution and tumor uptake of the ^{99m} Tc-labeled complex was studied in Ehrlich Ascite Tumor bearing mice. An injected dose of 100 µl of the ^{99m} Tc-labeled complex (3.7MBq) was administered through the tail vein of each mouse using 24" gauze needle. The mice were sacrificed at different time intervals and blood was obtained by cardiac puncture. The blood was weighed and radioactivity was measured in a shielded well gamma scintillation counter. The radioactivity present in the whole blood was calculated by keeping 7.3 % of the body weight as total body weight. Tissues (heart, lung, liver, spleen, kidney, stomach, intestine and tumor) were dissected, washed with normal saline, made free from adhering tissues, weighed and their radioactivity was measured in a shielded well gamma scintillation counter. To correct for physical decay and to calculate radiopharmaceutical uptake in each organ as a fraction of the injected dose, aliquots of the injectate, containing 2 % of the injected dose, were counted simultaneously at each time point.

Table 8.5. Organ/tissue concentrations of ^{99m}Tc-labeled Paclitaxel in Balb/c mice.

Organ/tissue	Percent injected dose per gram of organ/tissue (± SEM)				
	Plain Paclitaxel (PCL)				
	0.5 hour	1 hour	2 hour	4 hour	24 hour
Blood	12.13 ± 1.06	7.49 ± 0.58	3.59 ± 0.62	2.01 ± 0.47	0.02 ± 0.01
Heart	0.28 ± 0.09	0.24 ± 0.14	0.21 ± 0.11	0.18 ± 0.08	0.09 ± 0.05
Lung	3.12 ± 0.24	3.87 ± 0.89	3.62 ± 0.98	2.24 ± 0.82	1.88 ± 0.86
Liver	39.02 ± 2.43	37.34 ± 2.14	30.15 ± 2.26	25.42 ± 2.47	9.64 ± 1.96
Spleen	20.17 ± 2.18	18.68 ± 2.16	16.56 ± 2.04	11.49 ± 1.45	3.12 ± 1.01
Kidney	1.85 ± 0.38	1.9 ± 0.34	2.17 ± 0.56	2.06 ± 0.62	0.95 ± 0.33
Stomach	0.33 ± 0.11	0.36 ± 0.11	0.22 ± 0.14	0.1 ± 0.05	0.08 ± 0.04
Intestine	0.16 ± 0.08	0.13 ± 0.05	0.21 ± 0.06	0.12 ± 0.05	0.06 ± 0.03
Tumor	0.11 ± 0.04	0.16 ± 0.08	0.15 ± 0.06	0.15 ± 0.07	0.10 ± 0.04
Muscle	0.10 ± 0.03	0.11 ± 0.03	0.12 ± 0.04	0.12 ± 0.05	0.09 ± 0.02

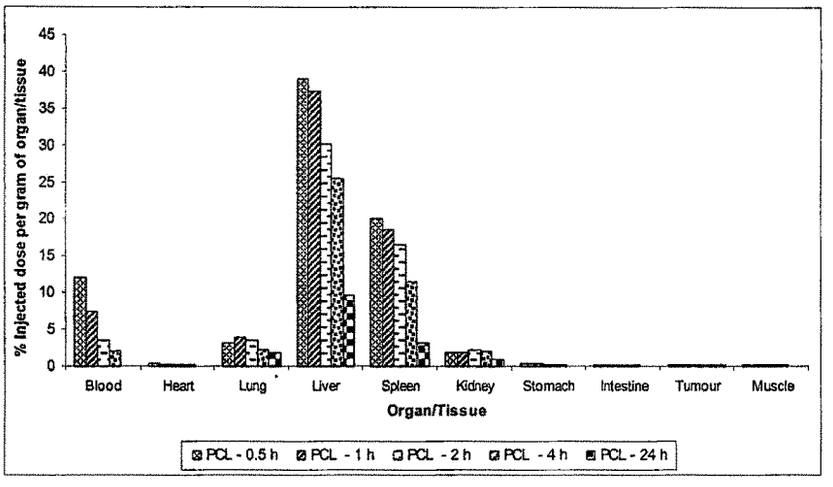

Figure 8.4. Organ/tissue concentrations of ^{99m}Tc-labeled Paclitaxel in Balb/c mice.

Table 8.6. Organ/tissue concentrations of ^{99m}Tc-labeled Conventional liposomes of Paclitaxel in Balb/c mice.

Organ/tissue	Percent injected dose per gram of organ/tissue (± SEM)				
	Conventional liposomes of Paclitaxel (CLPT)				
	0.5 hour	1 hour	2 hour	4 hour	24 hour
Blood	19.84 ± 1.64	17.02 ± 1.52	12.65 ± 1.44	10.64 ± 1.80	1.63 ± 0.74
Heart	0.16 ± 0.08	0.2 ± 0.08	0.21 ± 0.10	0.23 ± 0.10	0.11 ± 0.06
Lung	0.56 ± 0.09	0.92 ± 0.12	1.34 ± 0.23	0.68 ± 0.21	0.14 ± 0.08
Liver	25.12 ± 2.18	26.02 ± 2.54	23.16 ± 2.03	16.58 ± 1.82	10.69 ± 1.62
Spleen	12.32 ± 1.64	11.45 ± 1.45	7.21 ± 1.58	5.67 ± 1.68	2.09 ± 0.72
Kidney	1.05 ± 0.24	1.86 ± 0.42	1.74 ± 0.48	1.48 ± 0.52	0.57 ± 0.23
Stomach	0.28 ± 0.10	0.32 ± 0.14	0.41 ± 0.13	0.33 ± 0.18	0.14 ± 0.08
Intestine	0.23 ± 0.06	0.26 ± 0.07	0.28 ± 0.09	0.12 ± 0.04	0.05 ± 0.03
Tumor	0.17 ± 0.10	0.20 ± 0.09	0.27 ± 0.11	0.18 ± 0.07	0.16 ± 0.06
Muscle	0.13 ± 0.05	0.17 ± 0.07	0.12 ± 0.06	0.08 ± 0.04	0.08 ± 0.04

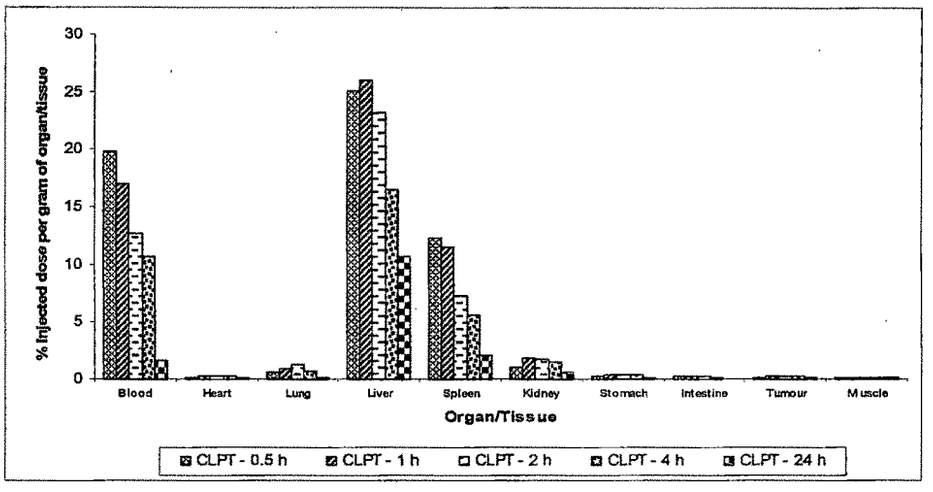

Figure 8.5. Organ/tissue concentrations of ^{99m}Tc-labeled Conventional liposomes of Paclitaxel in Balb/c mice.

Table 8.7. Organ/tissue concentrations of ^{99m}Tc-labeled pH sensitive liposomes of Paclitaxel in Balb/c mice.

Organ/tissue	Percent injected dose per gram of organ/tissue (± SEM)				
	pH sensitive liposomes of Paclitaxel (PSPT)				
	0.5 hour	1 hour	2 hour	4 hour	24 hour
Blood	36.46 ± 2.26	33.88 ± 2.41	32.11 ± 2.78	27.42 ± 2.14	14.77 ± 1.64
Heart	0.11 ± 0.06	0.12 ± 0.05	0.12 ± 0.05	0.16 ± 0.07	0.11 ± 0.04
Lung	0.48 ± 0.12	0.96 ± 0.24	1.24 ± 0.46	0.92 ± 0.32	0.22 ± 0.12
Liver	20.54 ± 2.16	20.71 ± 1.62	14.14 ± 1.46	12.73 ± 1.88	7.74 ± 0.98
Spleen	9.56 ± 1.02	9.84 ± 1.40	6.12 ± 1.34	4.45 ± 1.22	2.18 ± 0.52
Kidney	0.80 ± 0.34	0.88 ± 0.36	0.94 ± 0.24	0.85 ± 0.40	0.53 ± 0.21
Stomach	0.21 ± 0.14	0.23 ± 0.12	0.22 ± 0.14	0.21 ± 0.08	0.05 ± 0.02
Intestine	0.17 ± 0.06	0.21 ± 0.08	0.2 ± 0.08	0.18 ± 0.07	0.05 ± 0.03
Tumor	0.29 ± 0.11	0.65 ± 0.24	0.58 ± 0.20	0.52 ± 0.22	0.37 ± 0.18
Muscle	0.12 ± 0.08	0.07 ± 0.05	0.10 ± 0.05	0.10 ± 0.04	0.07 ± 0.03

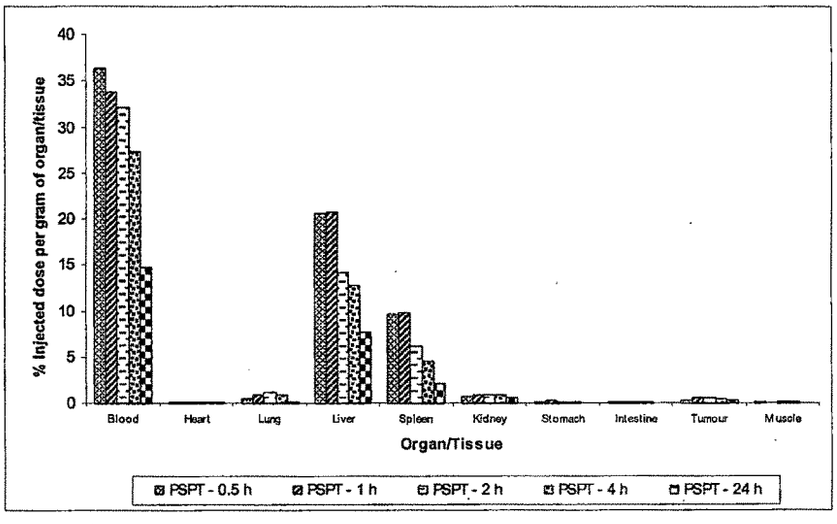

Figure 8.6. Organ/tissue concentrations of ^{99m}Tc-labeled pH sensitive liposomes of Paclitaxel in Balb/c mice.

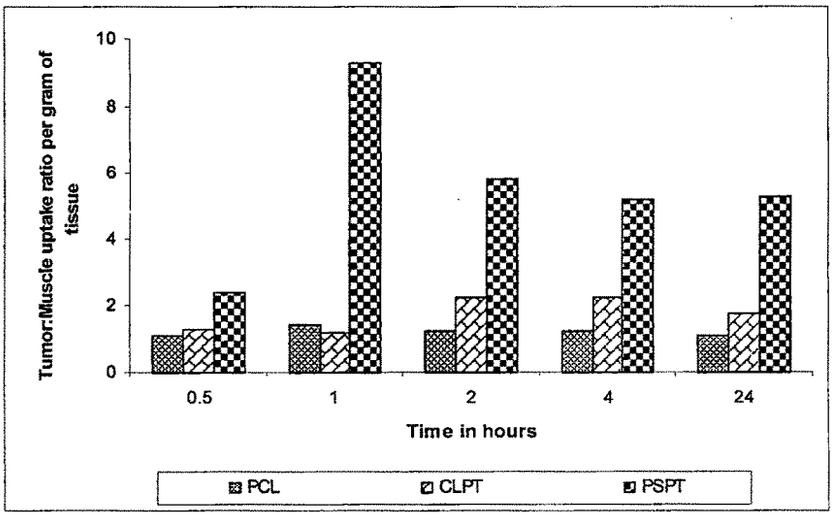

Figure 8.7. Tumor: Muscle ratio of PCL and its liposomal formulations

Table 8.8. Organ/tissue concentrations of ^{99m}Tc-labeled Irinotecan Hydrochloride in Balb/c mice.

Organ/tissue	Percent injected dose per gram of organ/tissue (± SEM)				
	Plain Irinotecan Hydrochloride (IH)				
	0.5 hour	1 hour	2 hour	4 hour	24 hour
Blood	10.65 ± 0.58	7.43 ± 0.38	3.67 ± 0.39	1.54 ± 0.30	0.03 ± 0.01
Heart	0.34 ± 0.12	0.31 ± 0.11	0.24 ± 0.08	0.18 ± 0.04	0.11 ± 0.05
Lung	3.51 ± 0.24	4.31 ± 0.82	3.97 ± 0.32	2.12 ± 0.18	1.52 ± 0.24
Liver	41.58 ± 2.48	37.88 ± 2.10	31.94 ± 2.43	27.56 ± 1.57	10.85 ± 1.45
Spleen	24.23 ± 2.12	24.46 ± 1.89	21.08 ± 1.59	14.78 ± 1.12	4.52 ± 0.86
Kidney	2.41 ± 0.59	1.90 ± 0.31	2.07 ± 0.13	2.37 ± 0.60	1.03 ± 0.17
Stomach	0.54 ± 0.18	0.43 ± 0.12	0.25 ± 0.14	0.07 ± 0.02	0.15 ± 0.09
Intestine	0.21 ± 0.08	0.12 ± 0.07	0.28 ± 0.05	0.17 ± 0.08	0.06 ± 0.06
Tumor	0.15 ± 0.07	0.19 ± 0.09	0.19 ± 0.05	0.16 ± 0.07	0.14 ± 0.03
Muscle	0.15 ± 0.06	0.10 ± 0.05	0.10 ± 0.06	0.16 ± 0.02	0.12 ± 0.03

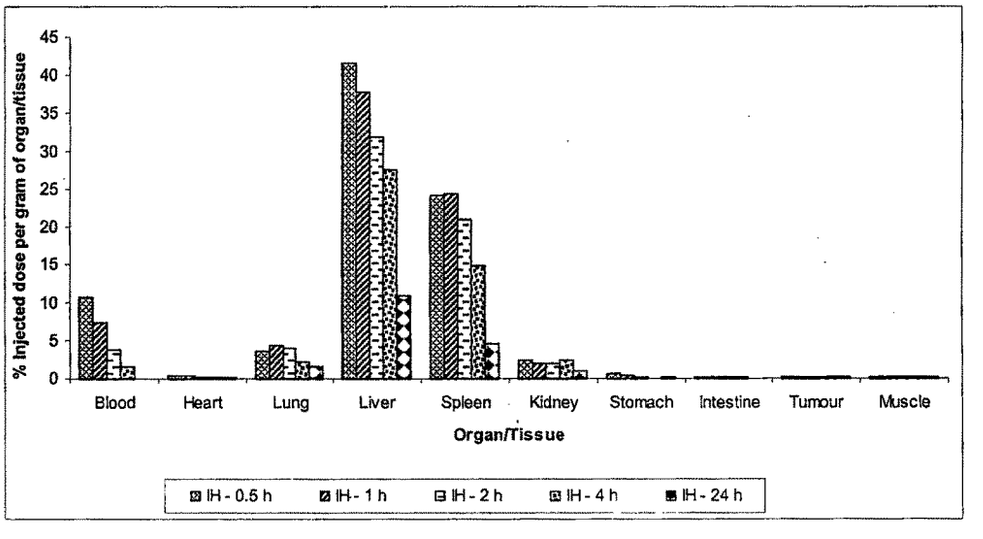

Figure 8.8. Organ/tissue concentrations of ^{99m}Tc-labeled Irinotecan Hydrochloride in Balb/c mice.

Table 8.9. Organ/tissue concentrations of ^{99m}Tc-labeled Conventional liposomes of Irinotecan in Balb/c mice.

Organ/tissue	Percent injected dose per gram of organ/tissue (± SEM)				
	Conventional liposomes of Irinotecan (CLIH)				
	0.5 hour	1 hour	2 hour	4 hour	24 hour
Blood	20.23 ± 0.48	17.06 ± 0.41	12.45 ± 0.50	9.68 ± 0.39	1.09 ± 0.21
Heart	0.18 ± 0.11	0.22 ± 0.13	0.25 ± 0.08	0.29 ± 0.04	0.13 ± 0.05
Lung	0.68 ± 0.28	1.08 ± 0.48	1.97 ± 0.30	0.75 ± 0.23	0.17 ± 0.11
Liver	25.97 ± 2.10	26.88 ± 2.34	23.21 ± 2.22	17.66 ± 1.67	11.02 ± 1.32
Spleen	12.87 ± 2.06	11.18 ± 1.67	10.30 ± 1.59	8.22 ± 1.43	3.67 ± 0.46
Kidney	1.45 ± 0.36	2.08 ± 0.37	1.54 ± 0.10	1.04 ± 0.68	0.42 ± 0.07
Stomach	0.24 ± 0.14	0.34 ± 0.12	0.31 ± 0.11	0.29 ± 0.06	0.10 ± 0.02
Intestine	0.32 ± 0.07	0.37 ± 0.06	0.36 ± 0.04	0.17 ± 0.04	0.04 ± 0.01
Tumor	0.18 ± 0.04	0.19 ± 0.08	0.26 ± 0.08	0.18 ± 0.03	0.18 ± 0.07
Muscle	0.11 ± 0.03	0.16 ± 0.05	0.11 ± 0.02	0.07 ± 0.02	0.08 ± 0.03

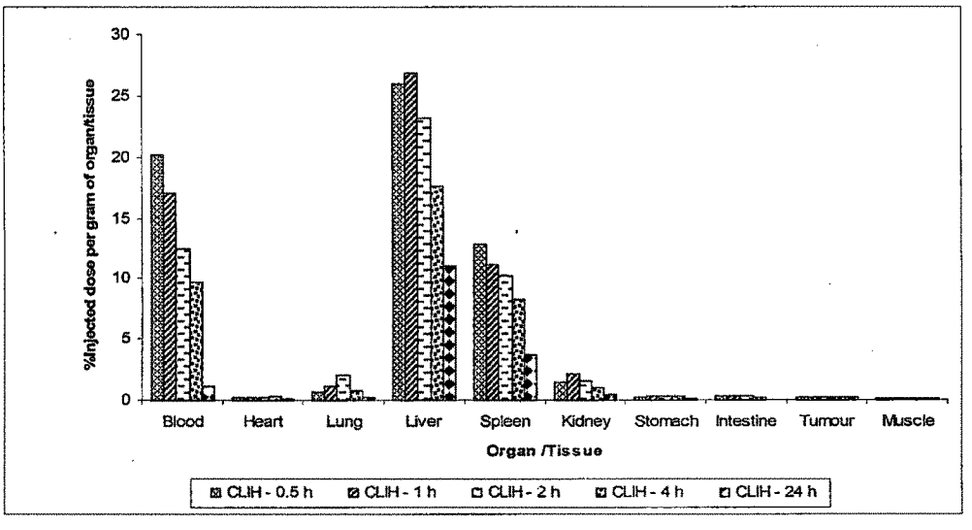

Figure 8.9. Organ/tissue concentrations of ^{99m}Tc-labeled Conventional liposomes of Irinotecan in Balb/c mice.

Table 8.10. Organ/tissue concentrations of ^{99m}Tc-labeled pH sensitive liposomes of Irinotecan in Balb/c mice.

Organ/tissue	Percent injected dose per gram of organ/tissue (± SEM)				
	pH sensitive liposomes of Irinotecan (PSIH)				
	0.5 hour	1 hour	2 hour	4 hour	24 hour
Blood	34.56 ± 0.65	31.45 ± 0.84	30.12 ± 0.55	26.12 ± 0.67	12.07 ± 0.28
Heart	0.12 ± 0.04	0.11 ± 0.03	0.13 ± 0.08	0.18 ± 0.06	0.13 ± 0.05
Lung	0.54 ± 0.20	1.04 ± 0.31	1.54 ± 0.30	0.86 ± 0.22	0.26 ± 0.12
Liver	23.97 ± 1.98	22.70 ± 2.18	22.64 ± 1.22	18.37 ± 1.45	8.61 ± 0.58
Spleen	10.28 ± 1.02	11.50 ± 1.14	11.67 ± 0.92	8.22 ± 0.64	2.37 ± 0.34
Kidney	0.98 ± 0.16	1.08 ± 0.37	1.08 ± 0.19	1.51 ± 0.48	0.83 ± 0.07
Stomach	0.25 ± 0.14	0.29 ± 0.10	0.26 ± 0.10	0.22 ± 0.05	0.04 ± 0.02
Intestine	0.27 ± 0.06	0.23 ± 0.04	0.20 ± 0.08	0.19 ± 0.02	0.06 ± 0.01
Tumor	0.28 ± 0.12	0.50 ± 0.08	0.58 ± 0.11	0.53 ± 0.13	0.28 ± 0.08
Muscle	0.12 ± 0.03	0.06 ± 0.03	0.10 ± 0.02	0.13 ± 0.06	0.06 ± 0.02

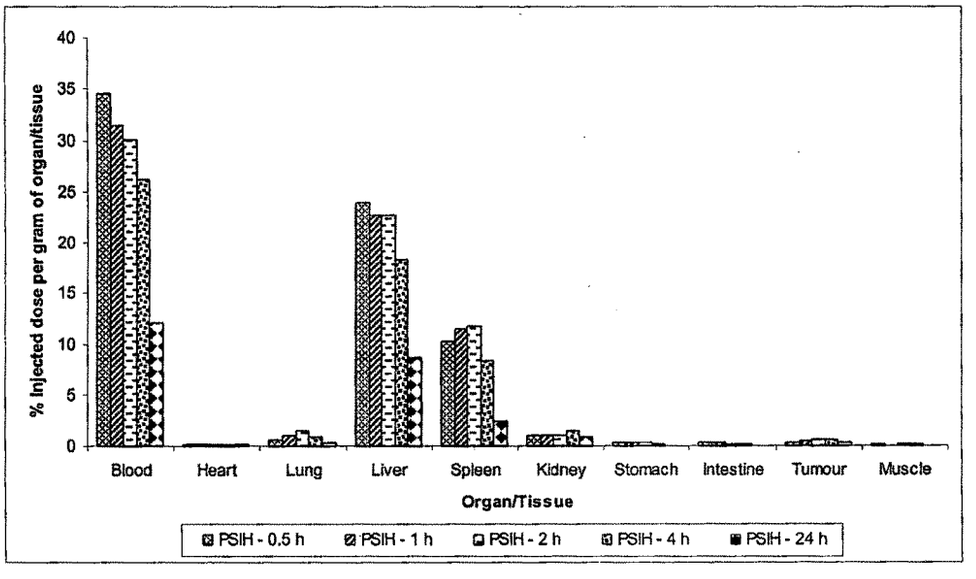

Figure 8.10. Organ/tissue concentrations of ^{99m}Tc-labeled pH sensitive liposomes of Irinotecan in Balb/c mice.

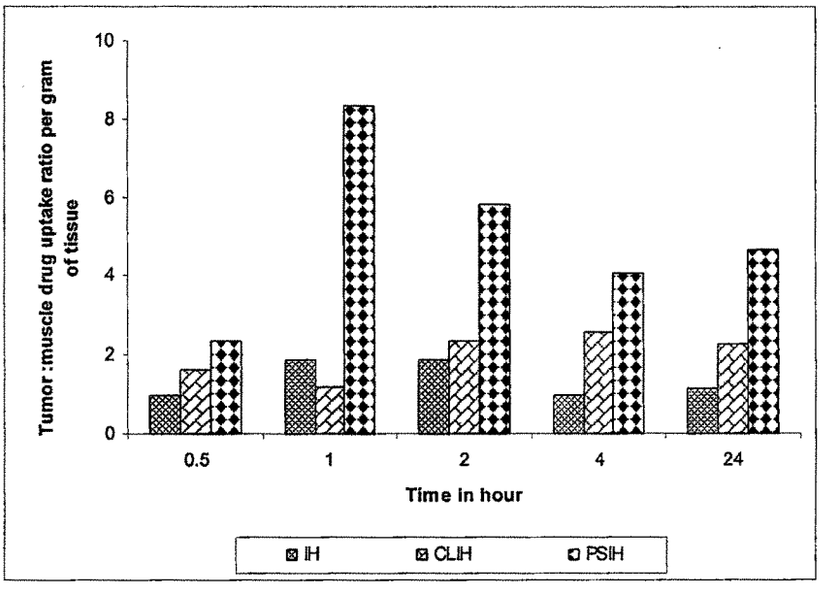

Figure 8.11. Tumor: Muscle uptake ratio for IH and its liposomal formulations.

8.5 Gamma Scintigraphy Imaging

Scintigraphic study was carried out in EAT bearing mice after administration of 3.7 MBq of ^{99m}Tc-labeled complex through the tail vein of mice. The mice were fixed on a board and imaging was performed using a single Photon Emission Computerized Tomography (SPECT, LC 75-005, Diacam, Siemens, USA) gamma camera. The gamma imaging photograph showing the biodistribution of PCL, Irinotecan and their liposomal formulations in EAT bearing mice is given in Figure 8.12 to 8.13.

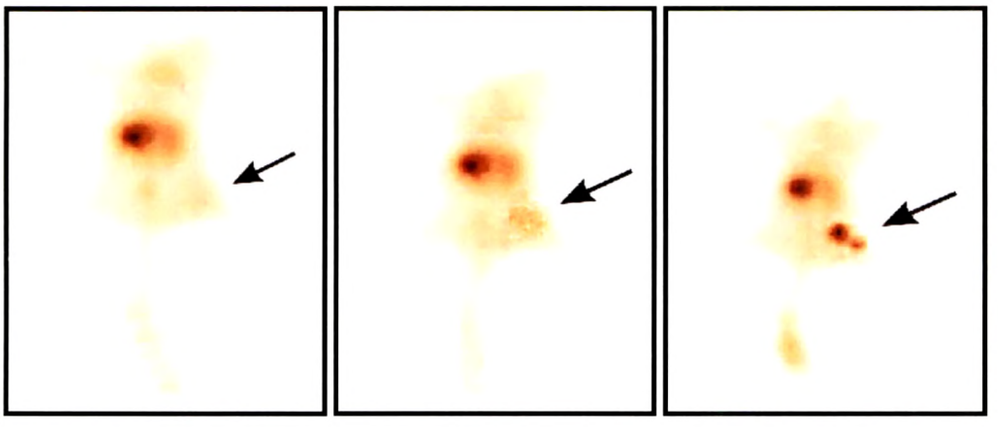

(a) (b) (c)

Figure 8.12. Gamma scintigraphic image of Plain Paclitaxel (a), conventional liposome of Paclitaxel (b) and pH sensitive liposome of Paclitaxel (c) after 1 hour of intravenous injection in tumor bearing Balb/c mice. The black portion in the figure represents radiolabeled complex.

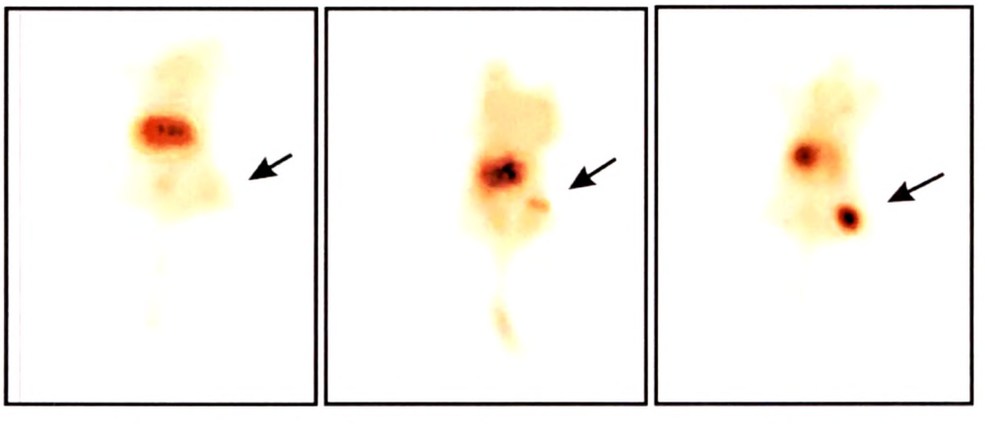

(a) (b) (c)

Figure 8.13. Gamma scintigraphic image of Plain Irinotecan (a), conventional liposome of Irinotecan (b) and pH sensitive liposome of Irinotecan (c) after 1 hour of intravenous injection in tumor bearing Balb/c mice. The black portion in the figure represents radiolabeled complex.

8.6 Data analysis

The data obtained above was subjected to statistical analysis using the WinNonlin 5.0.1 Validation Suite product, software (Pharsight Corporation, USA). The pharmacokinetic parameters generated by the analysis of the data obtained from blood kinetic study in mice are tabulated in table 8.2 and 8.4, respectively.

8.7 RESULTS AND DISCUSSION

The Paclitaxel and Irinotecan pH sensitive liposomes (PSPT and PSIH) were prepared with the aim of increasing blood circulation time and thereby increasing tumor targetability. This type of drug delivery would lead to drug action at the targeted site and significantly reduce the side effects, there by increasing therapeutic efficacy of the drug.

In-vivo testing of the prepared liposomes was performed by administering an appropriate volume of ^{99m}Tc-labeled pH sensitive liposomes through i.v. in Balb/c mice. The particle size of the liposomes maintained in a narrow range (preferably below 200nm) as reports suggests that high level of blood circulation is only observed for small liposomes of this range and larger than this size showed high level of accumulation in spleen with low concentration in blood circulation (Klibanov et. al., 1991). The very small liposomes of the range below 100nm might penetrate through fenestrations and gain access to hepatocytes because endothelial lining of the liver sinusoids includes fenestrae with an average diameter of 100 nm (Litzinger et. al., 1994: Wisse, 1970). The ^{99m}Tc-labeled drug or liposome complexes were injected into the tail vein of the Balb/c mice and measurement of the blood levels at predetermined time intervals was carried out. The data obtained was analyzed using WinNonlin 5.0.1 Validation Suite product, software (Pharsight Corporation, USA) to get an idea of blood kinetic profile of the drugs and liposomal formulations in mice. The Table 8.1 and 8.3 tabulate the raw data obtained from the experiment. Table 8.2 and 8.4 gives the pharmacokinetic parameters describing the *in-vivo* behaviour of the prepared liposomes generated by the analysis of the data. Figure 8.2 and 8.3 shows the comparison of the blood kinetics pattern of Paclitaxel and Irinotecan and their liposomal formulations respectively.

An appropriate volume of the radiolabeled complex was injected into the tail vein of the mice bearing Ehrlich Ascite Tumour (EAT) to determine the biodistribution pattern and the tumor targetability of the liposomal preparations. The mice were sacrificed at different time intervals and blood was obtained by direct cardiac puncture. Subsequently, other organ / tissues like heart, lung, liver, spleen, kidney, stomach, intestine, tumor and muscle were dissected out, washed in saline, dried using filter paper and the amount of labeled complex present in each organ / tissue was determined using gamma counter. The data so obtained was treated to analysis to get an idea of the kinetic profile of the drug / liposomal formulations in mice. The tables 8.5 to 8.10 tabulate the biodistribution data of the drug / liposomal formulations. The percent injected dose of the drugs and its liposomal formulations present in the whole organ or tissue is shown in the table 8.5 to 8.10. Figure 8.7 and 8.11 shows the comparison of tumor: muscle uptake ratio of PCL and IH with their liposomal formulations respectively.

Scintigraphic studies were carried out in EAT bearing mice after administration of an appropriate volume of the radiolabeled complex through the tail vein of Balb/c mice. The gamma imaging was performed using a Single Photon Emission Computerized Tomography (SPECT, LC 75-005, Diacam, Siemens, USA) gamma camera and are shown in Figures 8.12 and 8.13.

Paclitaxel (PCL) and its liposomes

The *in-vivo* data for plain drug and liposomal formulations of PCL on examination reveals that the liposomal formulations prolong the residence time of the drug in blood circulation. This observation is based on the value of the half-lives of the drug and the liposomes in mice (3.43 h for PCL, 8.48 h for CLPT and 27.74 h for PSPT, Table 8.2).

The pharmacokinetic parameters estimated for PCL and its liposomal formulations by using WinNonlin 5.0.1 Validation Suite product, software are summarized in Table 8.2. The area under the curve ($AUC_{0\text{-}48}$) values for PCL (35.67), for CLPT (142.43) and for PSPT (834.00) shows increased availability of the liposomal formulations CLPT (3.99 times) and PSPT (23.38 times) over the plain drug PCL respectively. The area under the curve ($AUC_{0\text{-}\infty}$) values for PCL (35.82), for CLPT (165.45) and for PSPT (1179.35)

shows increased availability of the liposomal formulation CLPT (4.62 times) and PSPT (32.92 times) over the plain drug PCL, which may be ascribed to the sustained release and the prolonged circulation of the liposomes. The reverse was observed for elimination rate constant (K_{el}) and volume of distribution (V_d).

The biodistribution of plain drug PCL was carried out in mice for a period of 24 hours. The amount of drug accumulated at the tumor site after 24 h was found to be as less as 0.10 % (Table 8.5)

Analysis of the organ distribution of the CLPT showed that these liposomes were predominantly distributed into liver and spleen (Table 8.6). This type of distribution is normally found with the non-sterically stabilized liposomes (Allen et. al., 1995). Thus CLPT behaved as expected *in-vivo*. There was an inverse relationship between liposome clearance by the reticuloendothelial system (RES) and a prolonged circulation time of liposomes as reported previously (Gabizon and Papahadjopoulos, 1988). In turn, there was a direct correlation between prolonged circulation time and liposome localization in tumor site.

The results of the *in-vivo* investigations of PSPT containing mPEG-DSPE showed extremely encouraging results with high elimination half life and high bioavailability (Table 8.7). This is in accordance with the reports published earlier, which acknowledge the superiority of mPEG derivatives over the other agents for steric stabilization of liposomes. These PSPT liposomes were present in the blood for an extended period of time as compared to the corresponding CLPT (1.63 % for CLPT where as 14.77% for PSPT at the end of 24 h, Table 8.6 and 8.7). The distribution of the PSPT to liver and spleen was considerably reduced as compared to CLPT and PCL. This indicates that PSPT successfully alters the distribution pattern as compared to the CLPT and PCL. After 24h, the PSPT achieved about 9 times more concentration in circulation as that of CLPT. The presence of very low amount of radioactivity in stomach after 24 h proved the *in-vivo* stability of the radiolabeled complexes. As the time increases from 0.5 h to 2 h accumulation of liposomes in tumor increases and the concentration decreases at 24 h.

The increase in accumulation at tumor site was also due to the increase in blood circulation time. Throughout the experimentation period, it was found that the distribution of PSPT to liver, spleen, tumor and blood varied significantly when compared to CLPT. The combination of lipids, presence of mPEG derivative and the particle size of the liposomes played a major role in tumor accumulation in case of PSPT. It has been postulated that decreased uptake of PSPT by MPS was possibly due to the presence of steric barrier, which decreases the adsorption of plasma proteins (opsonins) on the surface of liposomes. The pH sensitive liposome prepared with mPEG-DSPE showed higher blood concentration and long circulation time compared to CLPT which lacks it. From the Figure 8.7 which depicts the tumor: muscle uptake ratio of PCL and its liposomes, it was quite evident that the PSPT has got higher ratio than PCL and CLPT. It was found that PSPT attained more than 9 folds increased tumor accumulation than normal muscle after 1 h, 5.8 folds after 2 h, more than 5 folds after 4 h and 24 h when compared to 1.18 folds after 1 h, 2.25 folds after 2 h, around 2 folds after 4 h and 24 h treatment with CLPT. Plain PCL has shown much less tumor: muscle uptake ratio. Thus the avoidance of RES uptake and long circulation time increased accumulation in tumor site of PSPT is proved. The observation was supported by gamma scintigraphic images of EAT bearing mice (Figure 8.12). After 1 h, 2 h and 24 h of post injection of ^{99m} Tc labeled liposomal formulations, the gamma images were taken. This demonstrated the increased accumulation of PSPT in tumor present in the right thigh of the mice compared to CLPT and PCL at all time points.

Irinotecan (IH) and its liposomes

The *in-vivo* data for plain drug and liposomal formulations of IH on examination reveals that the liposomal formulations prolong the residence time of the drug in blood circulation. This observation is based on the value of the half-lives of the drug and the liposomes in mice (3.20 h for IH, 8.65 h for CLIH and 22.25 h for PSIH, Table 8.4).

The pharmacokinetic parameters estimated for IH and its liposomal formulations by using WinNonlin 5.0.1 Validation Suite product, software are summarized in Table 8.4. The area under the curve (AUC_{0-48}) values for IH (34.82), for CLIH (154.56) and for

PSIH (740.51) shows increased availability of the liposomal formulations CLIH (4.44 times) and PSIH (21.27 times) over the plain drug IH respectively. The area under the curve ($AUC_{0-\infty}$) values for IH (34.91), for CLIH (179.78) and for PSIH (958.15) shows increased availability of the liposomal formulation CLIH (5.15 times) and PSIH (27.45 times) over the plain drug IH, which may be ascribed to the sustained release and the prolonged circulation of the liposomes. The reverse was observed for elimination rate constant (K_{el}) and volume of distribution (V_d).

The biodistribution of plain drug IH was carried out in mice for a period of 24 hours. The amount of drug accumulated at the tumor site after 24 h was found to be as less as 0.14 % (Table 8.8) Analysis of the organ distribution of the CLIH showed that these liposomes were predominantly distributed into liver and spleen (Table 8.9). This type of distribution is normally found with the non-sterically stabilized liposomes (Allen et. al., 1995). Thus CLIH behaved as expected *in-vivo*. There was an inverse relationship between liposome clearance by the reticuloendothelial system (RES) and a prolonged circulation time of liposomes as reported previously (Gabizon and Papahadjopoulos, 1988). In turn, there was a direct correlation between prolonged circulation time and liposome localization in tumor site.

The results of the *in-vivo* investigations of PSIH containing mPEG-DSPE showed extremely encouraging results with high elimination half life and high bioavailability (Table 8.10). This is in accordance with the reports published earlier, which acknowledge the superiority of mPEG derivatives over the other agents for steric stabilization of liposomes. These PSIH liposomes were present in the blood for an extended period of time as compared to the corresponding CLIH (1.09 % for CLIH where as 12.07% for PSIH at the end of 24 h, Table 8.9 and 8.10). The distribution of the PSIH to liver and spleen was considerably reduced as compared to CLIH and IH. This indicates that PSIH successfully alters the distribution pattern as compared to the CLIH and IH.

After 24h, the PSIH achieved about 11 times more concentration in circulation as that of CLIH. The presence of very low amount of radioactivity in stomach after 24 h proved the

in-vivo stability of the radiolabeled complexes. As the time increases from 0.5 h to 2 h accumulation of liposomes in tumor increases and the concentration decreases as the time tends to 24 h. The increase in accumulation at tumor site was also due to the increase in blood circulation time. Throughout the experimentation period, it was found that the distribution of PSIH to liver, spleen, tumor and blood varied significantly when compared to CLIH. The combination of lipids, presence of mPEG derivative and the particle size of the liposomes played a major role in tumor accumulation in case of PSIH. It has been postulated that decreased uptake of PSIH by MPS was possibly due to the presence of steric barrier, which decreases the adsorption of plasma proteins (opsonins) on the surface of liposomes. The pH sensitive liposome prepared with mPEG-DSPE showed higher blood concentration and long circulation time compared to CLIH, which lacks it. From the Figure 8.11 which depicts the tumor: muscle uptake ratio of IH and its liposomes, it was quite evident that the PSIH has got higher ratio than IH and CLIH. It was found that PSIH attained more than 8 folds increased tumor accumulation than normal muscle after 1 h, 5.8 folds after 2 h, more than 4 folds after 4 h and 24 h when compared to 1.19 folds after 1 h, 2.36 folds after 2 h, more than 2 folds after 4 h and 24 h treatment with CLIH. Plain IH has shown much less tumor: muscle uptake ratio. Thus the avoidance of RES uptake and long circulation time increased accumulation in tumor site of PSIH is proved. The observation was supported by gamma scintigraphic images of EAT bearing mice (Figure 8.13). After 1 h, 2 h and 24 h of post injection of ^{99m} Tc labeled liposomal formulations, the gamma images were taken. This demonstrated the increased accumulation of PSIH in tumor present on the right thigh of the mice compared to CLIH and IH at all time points.

8.8 CONCLUSIONS

The rapid elimination of plain drugs and conventional liposomes encapsulated with anticancer drugs proved their inability to prolonged circulation in blood and thereby, decreased tumor accumulation. mPEG derivative used in the preparation of pH sensitive liposomes imparted sufficient steric stabilization, which lead to increased blood circulation and tumor accumulation. This enhanced circulation and increased tumor accumulation will greatly help to tackle solid tumors.

8.9 REFERENCES

Allen, T. M., Hansen, C., Lopez de Menezes, D. (1995) Pharmacokinetics of long circulating liposomes. *Adv. Drug. Deliv. Rev.* **16**: 267- 284.

Gabizon, A., Papahadjopoulos, D. (1988) Liposome formulations with prolonged circulation time in blood and enhanced uptake by tumours. *Proct. Natl. Acad. Sci. USA.* **85**: 6949 – 6953.

Klibanov, A.L., Maruyama, K., Beckerleg, A.M., Torchilin, V.P., Huang, L. (1991) Activity of amphipathic poly(ethylene glycol) 5000 to prolong the circulation time of liposomes depends on the liposome size and is unfavourable for immunoliposome binding to target. *Biochim. Biophys. Acta.* **1062**: 142-148.

Litzinger, D.C., Buiting, A.M.J., Rooijen, N.V., Huag, L. (1994) Effect of liposome size on the circulation time and intra organ distribution of amphipathic poly(ethylene glycol)-containing liposomes. *Biochim. Biophys. Acta.* **1190**: 99-107.

Wisse, E. (1970) An electron microscopic study of the fenestrated endothelial lining of rat liver sinusoids. *J. Ultrastruc. Res.* 31: 125-150.

Wu, M. S., Robbins J.C., Ponpipom, M. M., Shen, T.V. (1981) Modified *in-vivo* behaviour of liposomes containing synthetic glycolipids. *Biochim. Biophys. Acta.* **674**: 19-29.